Morphology and Physical Properties of Closed Cell Microcellular Ethylene–Octene Copolymer: Effect of Precipitated Silica Filler and Blowing Agent

N. C. NAYAK, D. K. TRIPATHY

Rubber Technology Centre, Indian Institute of Technology, Kharagpur 721 302, India

Received 21 December 2000; accepted 23 April 2001

ABSTRACT: The morphology of the microcellular ethylene–octene copolymer (Engage) of both unfilled and precipitated silica-filled compounds was studied from SEM photomicrographs with variation of blowing agent and silica filler loading. The average cell size, maximum cell size, and cell density varies with variation of blowing agent and filler loading. Physical properties similar to relative density, hardness, tensile strength, elongation at break, modulus, and tear strength decreases with blowing agent concentration. The elastic nature of closed cells reduces the hysteresis loss compared to solid compounds. Set properties improve with blowing agent concentration. It is observed that stress relaxation behavior is independent of blowing agent loading (i.e., density of closed cell microcellular vulcanizates). Theoretically, flaw sizes are found to be about 3.08 times larger than maximum cell sizes observed from SEM photomicrographs.
 J Appl Polym Sci 83: 357–366, 2002

Key words: ethylene–octene copolymer; microcellular POE; silica filler; blowing agent; morphology

INTRODUCTION

Polyolefin foams have penetrated the automotive, packaging, building and construction, marine, medical, sports, and leisure markets because of their wide variety of properties such as light weight, chemical resistance, inertness, buoyancy, good aging, cushioning performance, thermal and acoustic insulation, and recyclability.[1] Crosslinked polyolefin foams possess tremendous potential but they do not provide a high enough state of physical properties at a given flexibility to fully compete with the cellular elastomer market. Polyolefin resin made with conventional catalyst technology exhibits relatively wide molecular weight distribution and nonuniform branch structure. This nonuniformity contributes to the inability of polyolefins to provide the high state of physical properties offered by cellular elastomer.[2] In 1993, DuPont–Dow Elastomer introduced polyolefin elastomers (POEs) under the brand name Engage. They are ethylene–octene copolymers produced via advanced INSITE™ catalyst and process technology designed to be processed similar to thermoplastic but can be compounded similar to elastomers.[3] The exceptional performance of Engage is attributed to extraordinary control over polymer structure, molecular weight distribution, uniform comonomer composition, and rheology. They are being considered for use in diverse applications such as cushioning agents and gaskets, and particularly, as a good alternative for sealing application because of their structural regularity and nontoxic composition. Foam made

Correspondence to: D. K. Tripathy (dkt@rtc.iitkgp.ernet.in).

Journal of Applied Polymer Science, Vol. 83, 357–366 (2002)

Table I Formulations of Unfilled and Silica-Filled Vulcanizates

Mix No.	G_0	G_2	G_4	G_6	ES_1	ES_2	ES_3	ES_4	ES_5	ES_6	ES_7	ES_8
Engage	100	100	100	100	100	100	100	100	100	100	100	100
Silica	0	0	0	0	30	30	30	30	45	45	45	45
Paraffin oil	2	2	2	2	9	9	9	9	12	12	12	12
ADC-21	0	2	4	6	0	2	4	6	0	2	4	6
DEG	—	—	—	—	2	2	2	2	3	3	3	3

Each mix contains ZnO, 3; stearic acid, 1; and dicumyl peroxide (DCP 98%), 1.2 phr.

from these metallocene-based polyolefins has recently been commercialized.[4] However, industrial and commercial applications of microcellular elastomers demand strong, smooth skin and uniform cell structure. Close control of foam structure depends on the proper selection of blowing agents and curatives to achieve the correct balance between gas generation and degree of cure. The morphology of elastomeric foams[5] and characterization of microcellular foam[6] have also been reported. Mechanical properties and modeling of cellular materials of polymers, ceramics, and metals have been published by several authors.[7–9] Theoretical modeling of elastomeric latex foam has been developed by some researchers for both open and closed cell foam to predict the failure properties.[10–13] The mechanism of nucleation and bubble growth in elastomers,[14] thermoplastics,[15] thermoplastic elastomers,[16] and microcellular thermoplastics[17–19] using blowing agent and supersaturated methods have been the subject of recent research. Recently, morphological and physicomechanical properties of cellular and microcellular rubbers such as hysteresis, damping, cell size, and thermal insulation properties have been reported.[20–26] This article reports the processing and compounding technique of producing closed cell microcellular POE, Engage, with uniform cell distribution. The morphology and physicomechanical properties with special reference to the effect of blowing agent and silica-filler loading were investigated.

EXPERIMENTAL

Materials

Engage-8150 (ethylene–octene copolymer) containing 25 wt % octene monomer with a melt flow index of 0.5 g/10 min (190°C/2.16 kg), density of 0.868 g/ml, and Mooney viscosity of ML_{1+4} (121°C) 35 (manufactured by DuPont–Dow Elastomer Co., USA) was used. The filler used was precipitate silica, manufactured by Degussa AG, Huerth, Germany, having specific gravity, 2; BET surface area, 160–120 m^2/g; and particle size, 10–20 nm. The dicumyl peroxide (DCP) used was of 98% purity, manufactured by Aldrich Chemical Co., Milwaukee, WI. The blowing agent used was azodicarbonamide (ADC) 21, manufactured by High Polymer Lab., New Delhi, India. The diethylene glycol (DEG; E. Merck, Mumbai, India) used was of a density of 1.115 g/ml.

Compounding and Sample Preparation

Engage was compounded with the ingredients according to the formulations of the mixes (Table I). Compounding was done in a Brabender Plasticoder (model PLE 330) having cam-type rotors. The engage was first melted at 80°C with a rotor speed of 60 rpm for 2 min, after which other ingredients were added. With subsequent incorporation of filler, mixing was continued for another 3 min to ensure homogeneous distribution of ingredients. In the case of filled compounds, blowing agent was added along with the filler for good dispersion. Finally, curative was added. The hot mix was taken out and passed through a tight nip two-roll mill to form a sheet. Cure characteristics of the vulcanizates were determined in a Monsanto rheometer R-100. The vulcanizates were molded at 160°C to 80% of their respective optimum cure times in an electrically heated hydraulic press at a pressure of 5 MPa. All the sides of the mold were tapered to 30° to facilitate the expansion of the microcellular product and for better mold release. Expanded microcellular sheets were postcured at 100°C for 1 h in an electrically heated air oven.

Test Procedures

Densities of the samples were determined according to ASTM D 3574-86. Hardness was measured

Table II Rheometric Characteristics of Unfilled and Silica-Filled Vulcanizates

Mix No.	Mooney Viscosity [$ML_{1+4\ 100}$°C]	Minimum Rheometric Torque (dN m)	Maximum Rheometric Torque (dN m)	Rheometric Scorch Time at 160°C (min)	Optimum Cure Time at 160°C (min)
G_0	48	8.5	46	1.25	18
G_2	48	8	38	1.25	18.5
G_4	47	8	28	1.5	19
G_6	46	8	19	1.5	21
ES_1	58	16.5	50	1.25	22
ES_2	57	16	44	1.25	22.5
ES_3	56	15.5	32.5	1.5	22.5
ES_4	56	15	26	1.5	23
ES_5	65	20.5	49	1.25	23
ES_6	63	20	43.5	1.25	23.5
ES_7	62	19	30	1.5	23.5
ES_8	61	18	30	1.5	24

by using a Shore A durometer as per ASTM D 676-59 T. Stress–strain properties similar to tensile strength, elongation at break, modulus, and hysteresis were determined on a Zwick universal testing machine at room temperature (25 ± 2°C) according to ASTM D 3574-86. Crescent tear strength and trouser tear strength were also measured in the Zwick as per ASTM D 3574-86. Stress relaxation was measured according to ASTM D 3574. Mooney viscosity was determined according to ASTM D1446-1963 by using a Negretti automatic shearing viscometer, model MK-III, UK. At least three samples were tested for each property and the mean values were reported.

SEM studies were carried out for determination of cell structure by using a JEOL JSM 5800 scanning electron microscope. Razor-cut surfaces from microcellular sheets as well as fractured surfaces of the tensile specimen were used as samples for SEM studies. The samples were gold coated before being studied.

RESULTS AND DISCUSSION

Rheometric Characteristics

The cure characteristics of the vulcanizates containing a blowing agent and a silica filler, obtained from Monsanto Rheographs, are summarized in Table II. It is seen that in both unfilled and silica-filled systems maximum rheometric torque decreases with an increase in blowing agent concentration. This decrease in maximum torque is due to decomposition of blowing agent and the decomposed gas forms microbubbles. These microbubbles reduce the melt viscosity and hence maximum torque decreases. With incorporation of filler, minimum rheometric torque increases but the maximum rheometric torque decreases marginally. However, there is significant change in Mooney viscosity values. Rheometric scorch time (t_2) increases marginally with increasing blowing agent concentration and filler loading. The optimum cure time increases with an increase in blowing agent and filler concentration. Curing is affected by the exothermic decomposition of the blowing agent. So, from rheographs, actual cure characteristics cannot be obtained but the resultant effect of curing and blowing can be obtained.

Morphology of Razor-Cut Surfaces

The SEM photomicrographs of various unfilled and silica-filled microcellular vulcanizates are shown in Figure 1. Quantitative image analysis was used to analyze the photomicrographs to determine the average cell size[27] or diameter. Maximum cell size and cell density (number of cells per unit volume) were also determined. The shape anisotropy ratio (R) was estimated from the values of the cell sizes along the principal directions.[7] The results are summarized in Table III. It is seen that average cell size decreases with increasing blowing agent loading as well with the increase in silica-filler loading. However, maximum cell size increases with increasing filler loading. It is observed that addition of filler in-

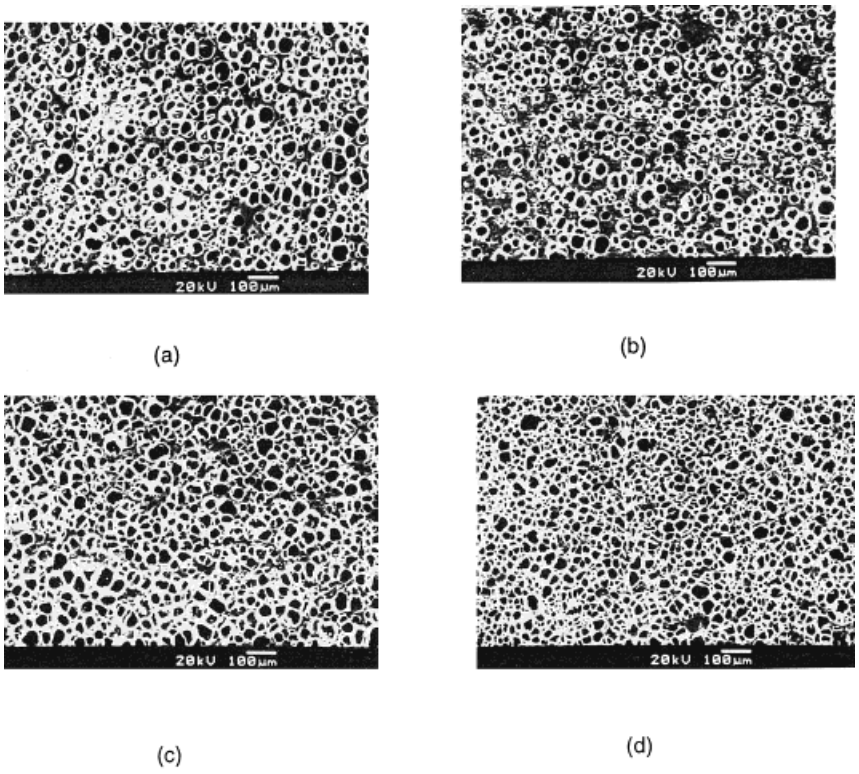

Figure 1 SEM photomicrograph of razor cut surfaces of microcellular Engage vulcanizates: (a) G_4; (b) ES_2; (c) ES_6; (d) ES_7.

creases the number of cells and also reduces the average cell size. An increase in the number of cells may be considered to be due to the nucleation by filler surfaces, and a decrease in cell size is attributed to an increase in melt viscosity by incorporation of silica filler, which retards the growth of cells. The number of cells per unit volume (m^{-3}) of the microcellular vulcanizates at maximum expansion is calculated by using the relation[5]

$$N = 6/\pi d^3[\rho_s/\rho_f - 1] \quad (1)$$

where N is the number of cells per unit volume; d is the average cell diameter; and ρ_s and ρ_f are the density of the solid and microcellular Engage vulcanizates, respectively. Figure 2 shows the variation of cell density with blowing agent loading for unfilled as well as filled vulcanizates. It is seen that cell density increases with increasing blowing agent. With incorporation of filler, the cell

Table III Physical Properties of Unfilled and Silica-Filled Vulcanizates

Mixes	Relative Density $[\rho_f/\rho_s]$	Hardness (Shore A) [μm]	Average Cell Size [μm]	Shape Anisotropy Ratio (R)	Maximum Cell Size [μm]	Cell Density $N = 6/\pi d^3[\rho_s/\rho_f - 1]^{-3}$
G_2	0.722	50	27 ± 1.8	1.07	60	3.72×10^{13}
G_4	0.577	32	26 ± 1.7	1.11	60	7.9×10^{13}
G_6	0.477	22	23 ± 1.5	1.12	55	1.71×10^{14}
ES_2	0.725	62	26 ± 1.7	0.99	80	4.1×10^{13}
ES_3	0.451	35	25 ± 1.7	1.03	78	1.48×10^{14}
ES_4	0.381	28	20 ± 1.3	1.04	65	3.87×10^{14}
ES_6	0.488	44	25 ± 1.7	0.97	75	1.28×10^{14}
ES_7	0.402	33	24 ± 1.5	1.19	64	2.05×10^{14}
ES_8	0.307	22	19 ± 1.3	1.2	60	6.26×10^{14}

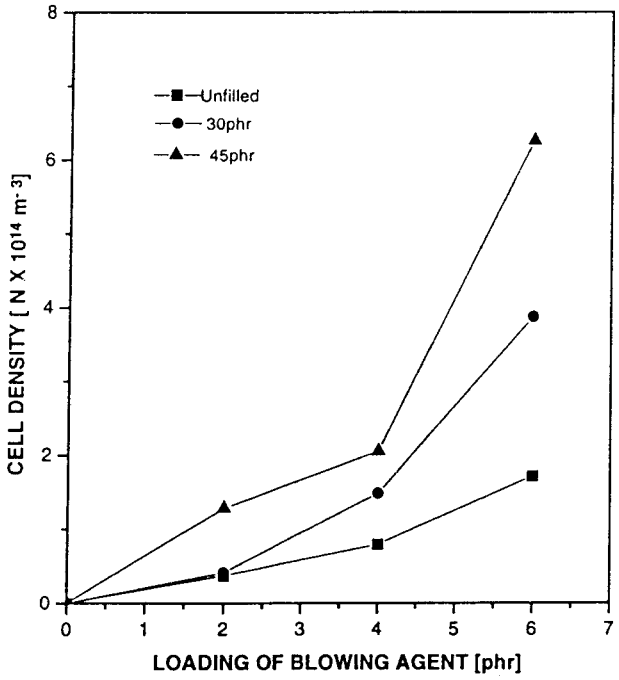

Figure 2 Cell density (N) of microcellular Engage vulcanizates: Effect of blowing agent and filler loading.

density is further enhanced, as has been explained above.

Physical Properties

Percentage of volume expansion of the Engage vulcanizates is shown in Figure 3. It is observed that the percentage of volume expansion increases with an increase in loading of both blowing agent and silica filler. Increase in percentage volume expansion is due to more decomposition of blowing agent and less diffusion of decomposed gas during curing. Physical properties similar to relative density and hardness are given in Table III. The relative density decreases with increasing blowing agent loading for both unfilled and filled vulcanizates. The hardness of the unfilled and filled closed cell microcellular POE decreases with increasing blowing agent loading. As the enclosed gas in the closed cell has little elastic property, hardness decreases with a decrease in relative density.

Tensile strength, elongation at break, modulus, and tear strength values are given in Table IV. Tensile strength, elongation at break, and modulus values decrease with increasing blowing agent loading. In the case of solid vulcanizates, tensile strength and elongation at break decreases with increasing concentration of filler loading but the modulus increases marginally. This can be attributed to the fact that because of high polar surface of silica filler, polymer-filler interaction is weak. Moreover, these rigid fillers can act as defects and stress raiser in the composites when the interfacial adhesion between filler and matrix is not strong,[28] which is the case with Engage and silica filler. Tear strength also decreases with increasing blowing agent loading in the case of both unfilled and silica-filled microcellular vulcanizates.

Figure 4 shows the relative modulus at different percentages of elongation and relative tensile strength (σ_f/σ_s) of 45 phr silica-loaded closed cell microcellular vulcanizates plotted against relative density (ρ_f/ρ_s). The relative modulus, 100, 200, and 300%, and relative tensile strength decrease linearly with a decrease in relative density. A similar trend is also obtained with 30 phr filler loading. The decrease in relative tensile strength is sharper than the decrease in relative modulus. The maximum flaw size (i.e., flaws) affects the tensile strength but not the modulus. Therefore, relative tensile strength behaves differently than the relative modulus. It is also observed that the 300% relative modulus shows higher values than 100 and 200% relative modulus. According to additive rule, if the modulus depends only on relative density, then it will fol-

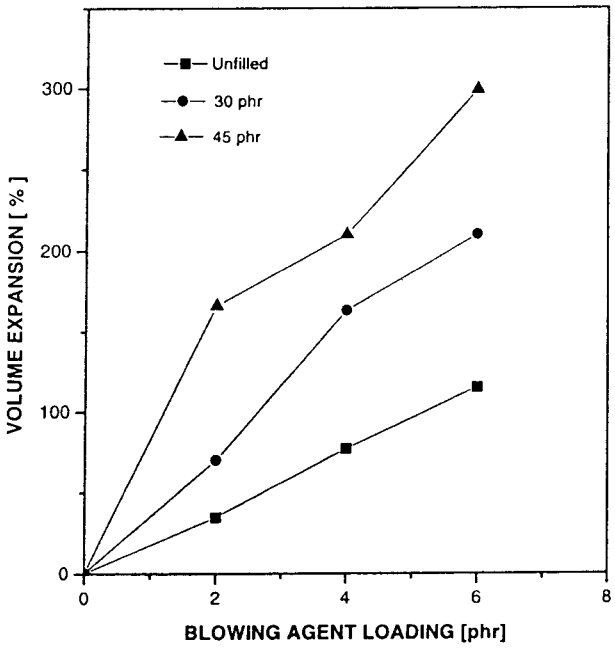

Figure 3 Variation of volume expansion (%) with blowing agent loading.

Table IV Physical Properties of Unfilled and Silica-Filled Microcellular Vulcanizates

Mix No.	Tensile Strength (MPa)	Elongation at Break (%)	Modulus (100%) (MPa)	Modulus (200%) (MPa)	Modulus (300%) (MPa)	Tear Strength (N/mm)
G_0	18.1	1157.7	2.23	2.96	3.6	35
G_2	4.2	573.2	1.51	2.13	2.7	24.5
G_4	3.4	501.3	1.12	1.72	2.31	19.38
G_6	2.7	406	0.94	1.5	2.10	13.6
ES_1	15	914.8	3.37	4.01	4.74	53.9
ES_2	7.9	674.4	2.36	3.21	3.99	34.51
ES_3	4.7	556.5	1.17	1.89	2.59	18.84
ES_4	3.3	485	0.80	1.43	2.04	14.13
ES_5	14.2	871.8	3.45	4.04	4.8	57.95
ES_6	5.9	566.7	1.7	2.56	3.33	25.8
ES_7	4.6	521.4	1.18	2.01	2.76	18.3
ES_8	2.9	442.94	0.81	1.46	2.05	12.42

low the line joining (0, 0) and (1, 1) points. Therefore, this increase in relative modulus may be due to an increase in enclosed gas pressure inside the cells.[25]

Figure 5 shows the hysteresis loss of 45 phr silica-filled solid and microcellular vulcanizates at 100% elongation. Table V summarizes the hysteresis loss values of different vulcanizates at 100% elongation. The hysteresis loss values of microcellular vulcanizates are found to decrease with an increase in blowing agent concentration. This is true for all cycles of measurement and at all filler loadings, whereas solid silica-filled vulcanizates exhibit increased hysteresis loss with incorporation of silica filler. This phenomenon may be attributed to the filler-rubber slippage mechanism.[29] The solid vulcanizates have higher hysteresis loss than their corresponding microcellular vulcanizates. The lower hysteresis loss values of microcellular Engage vulcanizates as com-

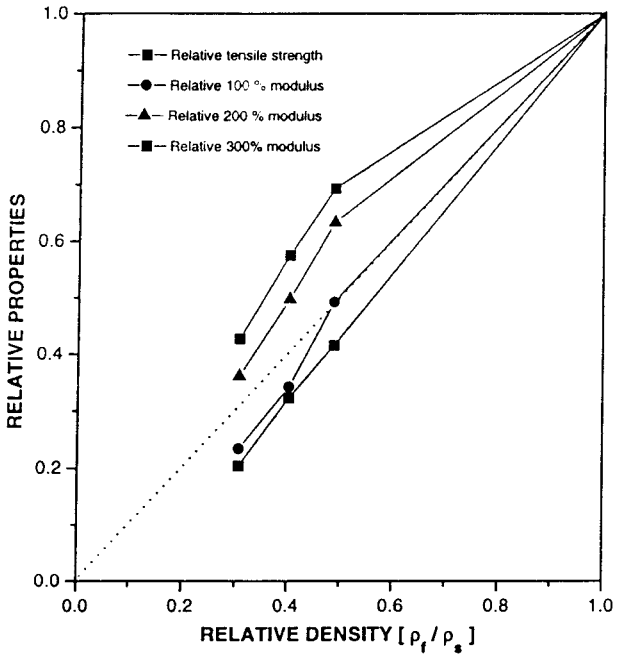

Figure 4 Effect of relative density (ρ_f/ρ_s) on relative properties of 45 phr silica-filled microcellular vulcanizates.

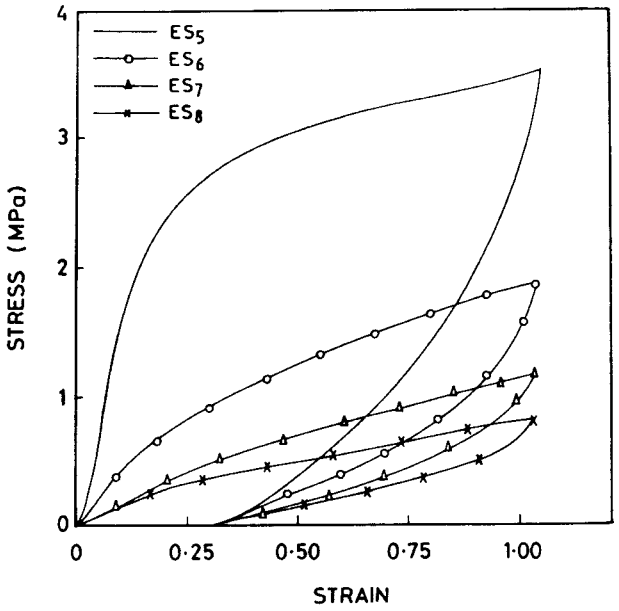

Figure 5 Hysteresis curves of 45 phr silica-filled vulcanizates.

Table V Result of Hysteresis Studies of Unfilled and Silica-Filled Microcellular Engage Vulcanizates

Mix No.	Hysteresis Loss in J/m^2 at 100% Elongation			% Set After 3rd Cycle
	1st Cycle	2nd Cycle	3rd Cycle	
G_0	0.035	0.022	0.018	6.6
G_2	0.028	0.015	0.013	5.6
G_4	0.021	0.011	0.010	4.4
G_6	0.018	0.009	0.008	3.4
ES_1	0.073	0.031	0.025	20
ES_2	0.043	0.020	0.017	13.3
ES_3	0.019	0.010	0.009	7.3
ES_4	0.012	0.006	0.005	6.6
ES_5	0.095	0.035	0.028	30
ES_6	0.034	0.017	0.015	15.3
ES_7	0.019	0.009	0.008	8.3
ES_8	0.013	0.006	0.005	7.6

pared to the solid vulcanizates and the decrease in hysteresis loss with an increase in blowing agent concentration can be attributed to the low-energy absorption values of closed cells. The percentage set of the microcellular vulcanizates after the third cycle in the hysteresis test were found to be lower than the solid vulcanizates. These percentage set values decreased with increasing blowing agent loading for a given filler loading and increased upon incorporation of silica filler at a particular blowing agent concentration. This phenomenon can be attributed to the highly resilient nature of the closed cell microcellular vulcanizates[23] due to gas pressure inside the cells.

The stress relaxation behavior of closed cell microcellular vulcanizates is determined by stretching the samples at a constant strain level of 100%. Figures 6 and 7 show the decay of stress with time for 30 and 45 phr silica-filled vulcanizates, respectively. Initially, the rate of decay is more prominent in the case of 45 phr silica-filled solid vulcanizates than that of 30 phr solid vulcanizates, which may be attributed to poor polymer–filler interaction. The nature of decay is almost similar to closed cell microcellular vulcanizates. Thus, the relaxation behavior is independent of blowing agent.[25–26]

Fracture Nuclei in Tensile Failure

The tearing energy of the foam, T_f, can be expressed as [10]

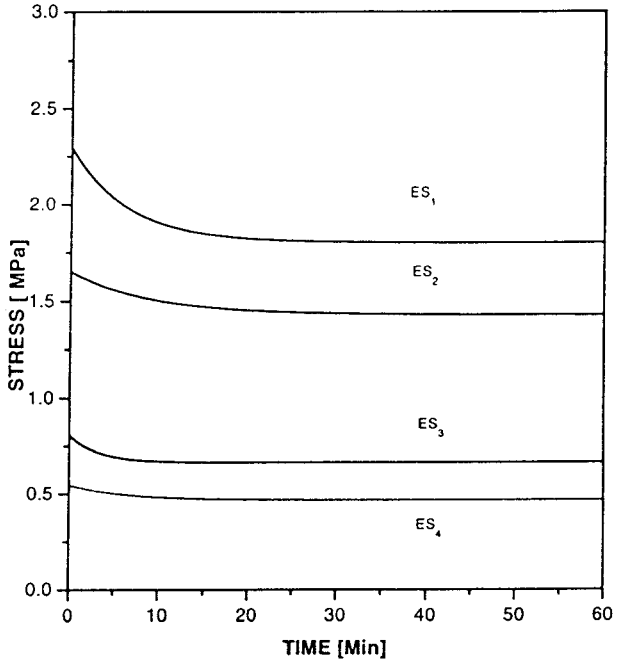

Figure 6 Stress relaxation behavior of 30 phr silica-filled closed-cell microcellular vulcanizates.

$$T_f = 2KE_f l \tag{2}$$

where K is a numerical constant having a value of about 2,[10] l is the depth of the flaw, and E_f is the

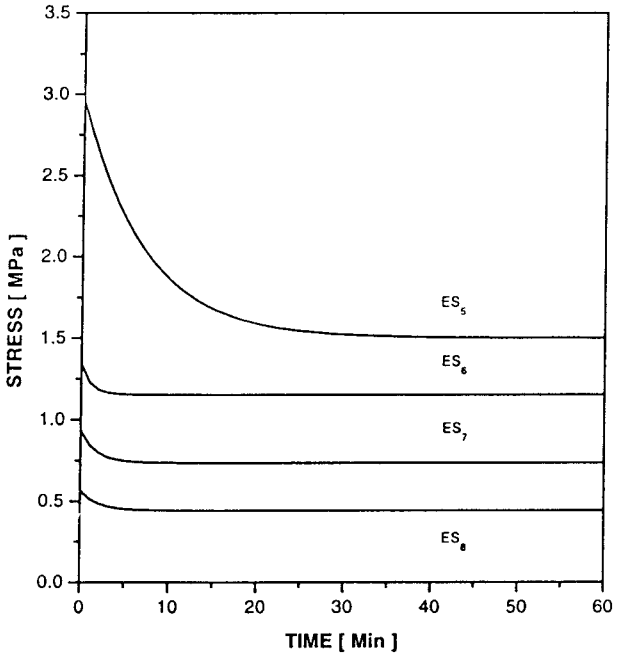

Figure 7 Stress relaxation behavior of 45 phr silica-filled closed-cell microcellular vulcanizates.

Table VI Tear Energy and Calculated Flaw Size of Unfilled and Silica-Filled Microcellular Engage Vulcanizates

Mix No.	Trouser Tear Resistance (N/mm)	Tear Energy (T_f) (KJ/m^2)	Strain Energy Density (KJ/m^2)	Calculated Cell Flaws (l) (μm)
G_2	4.79	9.58	12033	199
G_4	3.56	7.12	8517	208
G_6	1.77	3.54	5479	161
ES_2	19.91	39.82	26623	374
EC_3	3.92	7.84	13066	149
EC_4	2.61	5.22	8002	163
EC_6	10.57	21.14	16667	316
EC_7	3.86	7.72	11983	160
EC_8	1.76	3.52	6423	136

strain energy density at failure in the bulk of the test piece for the foam. According to tearing energy criterion developed by Rivlin and Thomas,[30] it can be assumed that tensile rupture occurs by catastrophic tearing of the flaw and is described in eq. 2. In the present work, the flaw depths of the microcellular Engage vulcanizates were calculated from eq. 2 by using the measured tear energy and strain energy density of the microcellular vulcanizates. The tear energy was calculated from the tear strength by using the trouser specimen (ASTM D-3574). The following equation was used for calculation of tear strength

$$T_f = 2 \times F/t$$

$$T_f = 2 \times T'_f \tag{3}$$

where T'_f is the trouser tear strength and T_f is the tear energy. Strain energy density can be calculated from the tensile strength and the elongation at the break of the dumbbell-shaped specimen. The results are summarized in Table VI. It is observed that theoretical values of the flaws depth (l) are larger than the corresponding maximum cell size. The mean value of the ratio of the theoretical depth of the flaws and the maximum cell size is about 3.08. According to Gent and Thomas,[10] for a perfectly regular foam structure, the tear tip diameter would be expected to be twice the pore diameter because of a random arrangement of pores in space. Imperfections in the foam will lead to local deviations of tear from a linear front and hence give rise to a corresponding larger effective diameter at the tip.

Tensile Fracture

Figure 8 demonstrates SEM photomicrographs of tensile fracture surfaces of silica-filled microcellular vulcanizates. Figure 7(a,b) shows the SEM fractograph of 30 and 45 phr silica-filled microcellular vulcanizates, respectively, having 4 phr blowing agent loading. Figures 7(c) and 7(d) show tensile fractographs of 30 and 45 phr silica-loaded vulcanizates, respectively, with 6 phr blowing agent. In all cases, it can be observed that the failure is catastrophic in nature, which leads to delamination. When tensile force is applied to the material, it is considered to be uniform throughout the tensile specimen, but concentration of stress builds up at the bigger cells. Failure starts at those points where the actual stress applied is much higher than the bulk of the specimen. Once the failure starts, it proceeds as catastrophic tear, giving rise to a layer surface with a number of tear lines.[31] In these cases, the layer delamination is prominent. When tensile force is applied to the material, it is also concentrated in the vicinity of the interfaces of filler particle and polymer matrix. In this region, the stress level is considerably higher than the average value.[32] Weak filler–polymer interaction also leads to formation of loose agglomerates in the matrix, which acts as a stress raiser[33] and provides an easy path for catastrophic failure.

CONCLUSION

1. In the case of microcellular Engage vulcanizates, the maximum rheometric torque

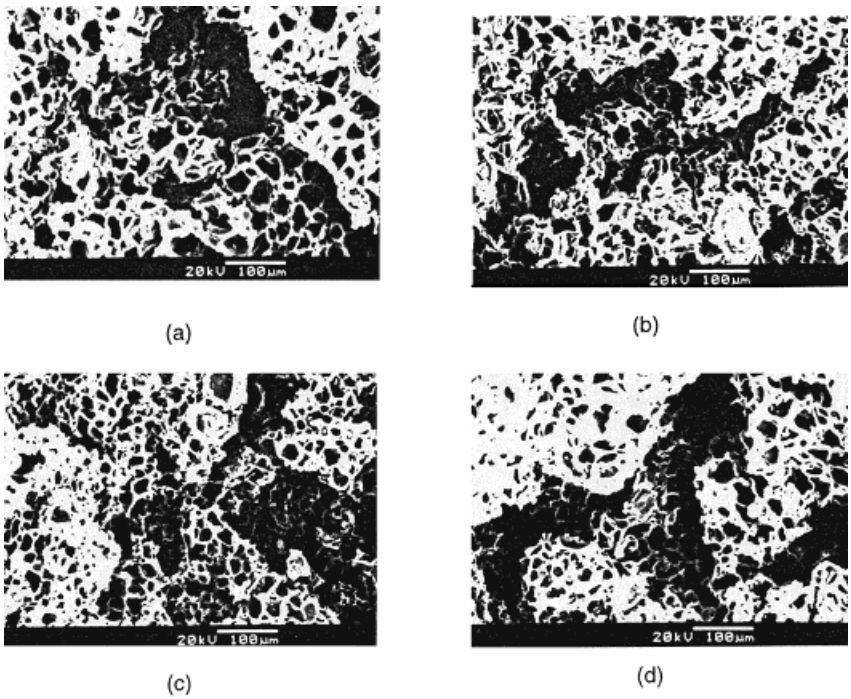

Figure 8 SEM photomicrograph of tensile fracture specimens: (a) ES_3; (b) ES_4; (c) ES_7; (d) ES_8.

decreases with an increase in blowing agent loading.
2. Average cell size decreases from 26 to 20 μm in 30 phr silica-filled and from 25 to 19 μm in 45 phr silica-filled vulcanizates with incorporation of 2–6 phr blowing agent.
3. Cell density and percentage volume expansion increases with increasing blowing agent loading as well as silica-filler loading. Thus, silica filler acts as nucleating agent.
4. Relative density decreases with increasing concentration of blowing agent.
5. Physical properties similar to tensile strength, elongation at break, and modulus decrease with increasing concentration of blowing agent.
6. Enclosed gas pressure in the closed cell increases the relative modulus in silica-filled vulcanizates, whereas relative tensile strength decreases sharply, which does not obey the additive rule.
7. The stress relaxation behavior is independent of blowing agent loading.
8. The hysteresis loss decreases with increasing blowing agent as well as filler loading.
9. Set properties are found to improve with increasing blowing agent concentration.
10. It is observed that theoretically calculated flaw sizes in tensile rupture is about 3.08 times larger than the maximum cell size measured from SEM photomicrographs, which suggests that tear path deviates from the linear front and gives rise to a larger effective depth of the flaws.
11. SEM fractograph studies of tensile fracture surfaces of microcellular vulcanizates reveal that the mechanism of fracture is dependent on the concentration of blowing agent and silica filler.

REFERENCES

1. Rodriguez-Perez, M. A.; Velasco, J. I.; Arencon, D.; Almanza, O.; De Saja, J. A. J Appl Polym Sci 2000, 75, 156.
2. Smith, S. C. Kautsch Gummi Kunstst 1998(7/8), 51, 504.
3. ENGAGE—A Polyolefin Elastomer; Manual; DuPont NEN: Wilmington, DE, 1996.
4. Huley, R. F.; Kozma, M. L.; Feichtinger, K. A. (to Sentinel Products Corp., Hyannis, MA) Eur. Pat. EP 0 702 032 A2, 1996.
5. Wang, C. S. J Appl Polym Sci 1982, 27, 1205.
6. Aubert, J. H. J Cell Plast 1988, 24(3), 132.

7. Gibson, L. J.; Ashby, M. F. Cellular Solids, Structure and Properties; Pergamon Press: Oxford, 1988.
8. Pakala, R. W.; Alviso, C. T.; Lemay, J. D. J Non-Crystal Solids 1990, 125, 67.
9. Gibson, L. J. Mater Sci Eng, A 1984, 110, 1.
10. Gent, A. N.; Thomas, A. G. J Appl Polym Sci 1959, 2(6), 354.
11. Gent, A. N.; Thomas, A. G. J Appl Polym Sci 1959, 1(1), 107.
12. Gent, A. N.; Thomas, A. G. Rubber Chem Technol 1963, 36, 597.
13. Lederman, J. M. J Appl Polym Sci 1971, 15, 693.
14. Stewart., C. W. J Polym Sci, Part A: Polym Chem 1970, 2, 8.
15. Exelby, J. H. Plast, Rubber Compos Process Appl 1991, 15(4), 213.
16. Dutta, A.; Cakmak, M. Rubber Chem Technol 1992, 65(5), 778.
17. Ramesh, N. S.; Rasmussen, D. H.; Cambell, G. A. Polym Eng Sci 1991, 31(23), 1657.
18. Cotton, J. S.; Suh, N. P. Polym Eng Sci 1987, 27(7), 493.
19. Kumar, V.; Suh, N. P. Polym Eng Sci 1990, 30(20), 1323.
20. Whitteker, R. E. J Appl Polym Sci 1971, 15, 1205.
21. Agarwal, P. D.; Kear, K. E. Rubber World 1990, 201(6), 20.
22. Hepburn, C.; Alam, N. Cell Polym 1991, 10(2), 99.
23. Mukhopadhyay, K.; Tripathy, D. K.; De, S. K. Rubber Chem Technol 1993, 66(1), 38.
24. Guriya, K. C.; Tripathy, D. K. Plast, Rubber Compos Process Appl 1995, 23(3), 195.
25. Guriya, K. C.; Tripathy, D. K. J Appl Polym. Sci 1996, 62, 117.
26. Nayak, N. C.; Tripathy, D. K. Cell Polym 2000, 19(4), 271.
27. Sims, G. L. A.; Khumiteekoh, C. Cell Polym 1994, 13, 137.
28. Demjen, Z.; Pukansky, B.; Nagy, J. Composites 1998, 29A, 323.
29. Harwood, J. A. C.; Mullin, L.; Pyne, A. R. J Appl Polym Sci 1965, 9, 3011.
30. Rivlin, R. S.; Thomas, A. G. J Polym Sci 1953, 10, 291.
31. Chakravarty, S. K.; De, S. K. Polymer 1983, 24, 1061.
32. Wypych, G. in Fillers; Chem Tec Publishing: Ontario, Canada, 1993; pp 203–205.
33. Mathew, N. M.; De, S. K. Polymer 1982, 23, 632.